



Published in final edited form as:

*Nat Cell Biol.* 2013 September ; 15(9): . doi:10.1038/ncb2832.

## A cost-benefit analysis of the physical mechanisms of membrane curvature

Jeanne C. Stachowiak<sup>1</sup>, Frances M. Brodsky<sup>2</sup>, and Elizabeth A. Miller<sup>3,\*</sup>

<sup>1</sup>Department of Biomedical Engineering, Institute for Cellular and Molecular Biology, University of Texas at Austin, Austin, TX 78712 USA

<sup>2</sup>Departments of Bioengineering and Therapeutic Sciences, Pharmaceutical Chemistry and Microbiology and Immunology, The G.W. Hooper Foundation, University of California, San Francisco, CA 94143 USA

<sup>3</sup>Department of Biological Sciences, Columbia University, New York, NY, 10027 USA

### Abstract

Many cellular membrane-bound structures exhibit distinct curvature that is driven by the physical properties of their lipid and protein constituents. Here we review how cells manipulate and control this curvature in the context of dynamic events such as vesicle-mediated membrane traffic. Lipids and cargo proteins each contribute energetic barriers that must be overcome during vesicle formation. In contrast, protein coats and their associated accessory proteins drive membrane bending using a variety of interdependent physical mechanisms. We survey the energetic costs and drivers involved in membrane curvature, drawing a contrast between the stochastic contributions of molecular crowding and the deterministic assembly of protein coats. These basic principles also apply to other cellular examples of membrane bending events, including important disease-related problems like viral egress.

### Introduction

Cellular membranes, which partition eukaryotic cells into distinct compartments, possess an intrinsic simplicity that belies their complex gymnastics during normal cellular function. The majority of cellular membranes are planar lipid bilayers. These are influenced by intrinsic and extrinsic forces to generate the curved structures that are associated with diverse cellular architectures (Figure 1). Curved membranes can be relatively stable structures - like those surrounding nuclear pores - or can be transient like transport vesicles that are continually produced and consumed during membrane and protein traffic. In each case, these structures form from the action of proteins that use distinct mechanisms to exert forces that sculpt the requisite membrane architecture<sup>1-3</sup>. Considerable insight into the mechanisms of membrane curvature has been gained from minimally reconstituted systems, largely based on shape changes exerted on synthetic liposomes by individual protein components. These systems have established that, in many instances, physical properties associated with a single protein are sufficient to induce curvature. In recent years, experimental systems have focused on two principles: membrane insertion and protein scaffolding. However, more recent theoretical and experimental analyses have suggested that molecular crowding is also an important driver of curvature, in a manner that can either augment the action of protein scaffolds, or oppose it. Finally, the effect of scaffold rigidity has also been raised as a key factor in contributing to membrane bending. Examples of each

\*corresponding author: em2282@columbia.edu.

of these types of curvature drivers can be found at different sites within the cell (Figure 1), where different bending requirements are likely specified by the lipid and protein composition of the underlying membrane.

The current challenge is to understand how the cooperative energetic contributions of multiple active components drive bending of complex membranes composed of diverse lipids and proteins. Cellular membrane bending also occurs in the context of organized tissue or in the face of turgor pressure, factors that introduce additional energetic barriers, necessitating additional force. Here we review the multiple physical mechanisms that influence membrane bending and perform an accounting of their relative energetic contributions to cellular membrane deformation. We focus primarily on vesicle trafficking pathways, although the same fundamental principles can also help us understand curvature in other cellular contexts. We first consider the physical properties of lipids and cargo, and the barriers they represent to membrane bending. We then discuss the drivers of membrane curvature and the different physical mechanisms that they employ. Together these considerations define an integrated set of parameters that operate during intracellular and plasma membrane bending. The energetic cost-benefit analysis that we describe here becomes particularly important in considering membrane curvature under pathological conditions, for example where pathogens induce uptake by cells, or when viruses bud from the plasma membrane, liberating themselves for additional rounds of infection.

## The energetic costs of bending a membrane

Most cellular phospholipids have a cylindrical shape and therefore self-assemble into planar bilayers. According to the simplified two-dimensional description of membrane mechanics by Canham<sup>4</sup> and Helfrich<sup>5</sup>, deforming bilayers into curved shapes encounters two energetic barriers: resistance to membrane bending and resistance to membrane stretching. As discussed below, bending rigidity generally poses the larger barrier to membrane curvature, except in cases where membrane tension is significantly raised by turgor pressure<sup>6</sup>, osmotic shock, or action of the cytoskeleton<sup>7</sup>. Many biological membranes, such as the plasma membranes of red blood cells<sup>8</sup> are thought to have significant spontaneous curvature, a preferred curvature<sup>5</sup> that typically arises from a difference in lipid composition between the two leaflets of the membrane<sup>9</sup>. Spontaneous curvature is likely to have a significant influence on the curvature of cellular structures, though this contribution remains difficult to quantify, since it arises from highly localized, often transient, differences in membrane composition.

## Cargo proteins

An under-appreciated player in the membrane-bending problem is the protein fraction embedded within the bilayer. Far from being inert vesicle passengers, cargo proteins represent major constituents of vesicles<sup>10</sup> that probably contribute a significant energetic barrier to membrane bending. As cargo concentration increases and membrane curvature progresses, the surface area available to each protein decreases on the concave, luminal membrane surface. This process increases steric repulsion among cargo molecules that can be expected to oppose membrane curvature (Figure 2A). Such effects are amplified when cargo proteins display asymmetry across the bilayer such that luminal domains are significantly larger than their corresponding cytoplasmic domains. An extreme example of this topology is the family of lipid-anchored proteins, glycosylphosphorylinositol (GPI)-anchored proteins. These abundant and diverse cell surface proteins expose their entire molecular mass on the luminal surface of transport vesicles<sup>11</sup>. Concentration of these proteins at budding sites may create significant lateral pressure within the membrane that could induce local negative (away from the membrane) curvature (Figure 2B).

The idea that unbalanced steric pressure among membrane-bound molecules can drive membranes to bend derives in part from the bilayer couple model of Sheetz and Singer<sup>12</sup>. These authors recognized that tight coupling between the two leaflets of a lipid bilayer engenders curvature whereby expanding or compressing one side of the membrane would cause the other side to experience the opposite effect (ie. compression or expansion). The increased abundance of molecules and the increased rate of collisions within or adjacent to one leaflet of the membrane causes the area of the leaflet to increase relative to the opposite leaflet, leading to membrane curvature away from the source of increased steric pressure (Figure 2B). The phenomenon of curvature driven by steric pressure has been demonstrated for synthetic membranes with a high concentration of polymer molecules attached to their outer surfaces<sup>13</sup>. More recently, it has been demonstrated that steric pressure between densely crowded, membrane-bound proteins can drive dramatic changes in membrane shape, forming narrow membrane tubules, even from stiff, solid-phase membranes<sup>14</sup>. In the first physiological example of this phenomenon, steric pressure between GPI-anchored proteins and other cargo molecules in the lumen of the endoplasmic reticulum appears to oppose the curvature enforced by the COPII vesicle coat machinery, driving a requirement for increased coat rigidity<sup>15</sup>. Similar costs are likely to apply to bona fide transmembrane cargo proteins, especially those with relatively small cytoplasmic domains like many surface receptors and Golgi glycosylation enzymes<sup>16</sup>.

## Overcoming the barriers to membrane bending

Cells have evolved multiple solutions to the problem of overcoming the energetic barriers associated with curving membranes (Figure 1). Early observations of clathrin-coated vesicles<sup>17</sup> and subsequent characterization of clathrin's self-assembling properties<sup>18</sup> gave rise to the long-standing premise that formation of spherical vesicles is driven by coat protein scaffolds that are capable of imposing their inherent curvature on membrane surfaces (Figure 1). In addition to the scaffolding effects of polymeric coat structures, further mechanisms that contribute to membrane bending have now been characterized. These include differential lipid and protein insertion into the bilayer, steric pressure among proteins bound to membrane surfaces, oligomerization of membrane-embedded and membrane-associated proteins, and actin polymerization. We consider each of these mechanisms in turn, starting with the membrane itself and working our way out towards the cytoplasm.

## Lipid asymmetry

Although the majority of membrane lipids are cylindrical in shape, lipids with large hydrocarbon tails (or small head groups) can take on a conical shape, and lipids with small tails (or large head groups) can adopt an inverse conical shape. The unequal distribution of such irregularly shaped lipids between the two leaflets of the membrane could impose a distinct curvature on the bilayer. Indeed, asymmetric lipids such as phosphatidylethanolamine and gangliosides<sup>19</sup> and ceramides<sup>20</sup> display curvature preferences. The asymmetric distribution of these lipids has been invoked to explain observations of curvature during autophagosome formation<sup>21</sup>. In the context of vesicle formation, local recruitment of lipases and other lipid-modifying enzymes, including flippases, may contribute to the curvature associated with vesicle formation<sup>22</sup>. Direct measurement of this effect in a cellular context has not been achieved, making the impact of lipid asymmetry difficult to quantify. Nonetheless, flippases are clearly implicated in post-Golgi trafficking events<sup>23</sup> and local release of sphingomyelinase can induce endocytosis<sup>24</sup> suggesting such mechanisms are physiologically relevant in cells.

## Protein asymmetry

In addition to the lipids themselves, asymmetric membrane insertion of proteins should also be capable of driving membrane bending according to the bilayer couple model<sup>25</sup>. Indeed, a number of cytosolic proteins that are central to membrane traffic, such as epsin1, Arf1 and Sar1, insert short amphipathic helices into one leaflet of the membrane when recruited. These proteins can tubulate synthetic liposomes when applied at relatively high concentrations<sup>26-29</sup>. However, whether it is physiologically possible to create a high enough local density of insertions to generate a significant driving force for membrane bending remains under debate<sup>30,31</sup>. Specifically, the physical dimensions of the proteins that contain insertable helices set a limit on the number of helices that can be actually be inserted at the membrane surface. As included in the analysis section below, even when all membrane-bound proteins insert helices, the membrane area occupied by helices cannot fill the disparity in area between the two leaflets of highly curved membranes. This analysis is based on the prediction by Campelo et al.<sup>30</sup> that insertions must cover at least 10% of the membrane surface area to drive formation of small vesicles. This situation is intractable except for cases in which proteins that contain multiple helix insertions cover the entire membrane surface<sup>30</sup>. Therefore hydrophobic insertion likely makes a relatively small contribution to the energy budget of membrane curvature in most settings. This is consistent with the formation of COPII-coated curved membranes in the absence of helix insertions<sup>27</sup> and curvature induced by clathrin and a truncated form of epsin that lacks the N-terminal amphipathic helix<sup>32</sup>.

An alternative effect that may account for the observed tubulation following recruitment of helix-containing proteins is steric pressure between densely crowded membrane-bound molecules. As described above with respect to asymmetric cargo proteins, this effect can itself drive membrane bending when the concentration of molecules is higher on one face of the membrane than the other. In this case, the crowding effect is achieved by local membrane association of coat assembly proteins, creating outward curvature and contributing to vesicle formation. Indeed, membrane-bound clathrin assembly proteins, including Epsin1 and AP180, have recently been demonstrated to drive bending of model membrane vesicles by creating steric pressure, accounted for by the reduced frequency of protein-protein collisions (ie. increased entropy) when the membrane bends away from its more densely crowded surface<sup>31</sup> (Figure 2D). Instead of driving bulk curvature, coat initiation by amphipathic-helix-containing proteins might generate initial local curvature but then couple this to coat propagation through recruitment of additional helix-containing (and other) proteins leading to steric pressure effects of the coat as a whole. Indeed, the amphipathic helix of Sar1 lowers the bending energy of the underlying lipid bilayer<sup>33</sup>, suggesting that it makes the membrane more susceptible to remodeling by downstream coat components<sup>25</sup>. Another function for amphipathic helices is detection rather than induction of curvature. This is almost certainly the case for the ALPS-domain of ARF-GAP, which detects lipid-packing defects in the curved bilayers of COPI vesicles, inserting specifically into membranes that are under curvature stress<sup>34</sup> and thus restricting its GTPase stimulation activity to curved membranes.

An extension of this protein asymmetry/molecular crowding model may also be relevant to cargo-driven vesiculation events. Experiments with membrane-bound polymers revealed that self-avoiding polymers create an expansive pressure that drives the membrane to bend away from them<sup>13,35</sup> (Figure 2B), a finding supported by a simple thermodynamic model<sup>36</sup>. Likewise, self-attracting polymers can be expected to create a compressive pressure that drives the membrane to bend toward them<sup>37</sup> (Figure 2C). Thus, vesiculation of the correct topology (that is towards the cytoplasm) might be induced by lumenally distributed proteins if they have affinity for each other. For example, apical sorting of GPI-anchored proteins

relies on their oligomerization<sup>38</sup>, raising the prospect that such sorting employs a cargo-driven budding event (Figure 2C). This phenomenon might also explain the biogenesis of secretory granules that have long been thought to employ a concentration-driven segregation mechanism of egress from the trans-Golgi network<sup>39</sup> (Figure 1), although the molecular details of the budding event are not yet fully defined. Viral budding may also employ such a mechanism whereby self-association of matrix proteins – driven in some cases by nucleic acid packaging – would couple with plasma membrane recruitment to drive outward budding of the enveloped virus<sup>40</sup> (Figure 1).

Cargo-driven molecular crowding effects could also be relevant to intracellular trafficking pathways for which cargo adaptors are known but no outer coat scaffold has been described. To date, no known coat mediates transport between the yeast TGN and plasma membrane, although some specialized cargo adaptors like exomer regulate selected transport steps<sup>41</sup>. Whether exomer recruits a more canonical coat scaffold remains to be seen. In a cargo-driven budding model, cargo concentration alone would create local shape changes in the membrane by virtue of molecular crowding (Figure 2B). In order for this model to work, a heterogeneous population of cargo proteins would require an asymmetric distribution in the membrane, with the bulk of their masses facing the cytoplasm. Alternatively, lumenally oriented cargoes would need to undergo significant inter-molecular interactions that would in turn change the spontaneous curvature of the underlying bilayer<sup>37</sup> (Figure 2C). Yet another alternative would invoke the molecular crowding effects of the cargoes plus their cargo adaptors such that the accumulated mass on the cytoplasmic face of the bilayer creates sufficient lateral pressure to bend the membrane in the desired direction (Figure 2D). Such a scenario might be accelerated by curvature-sensing properties of the cargo adaptors such that a positive feedback loop is created: local recruitment and concentration initiates curvature that is in turn sensed by additional adaptors that bring in additional cargo molecules, perpetuating the local curvature<sup>25</sup>. Indeed, such positive feedback may participate in the canonical coat systems where curvature may be induced initially by steric pressure among cargo adaptors, detected and propagated by accessory proteins with amphipathic helices and concave membrane-binding surfaces, further propagated and stabilized by cargo concentration and polymerization of a protein coat or the cargo adaptors themselves.

## Self-assembly of membrane-embedded proteins

Caveolins and reticulons are membrane-embedded proteins that undergo oligomerization to generate curvature<sup>42,43</sup> (Figure 1). They both have transmembrane domains that form wedge-shaped insertions with capacity to contribute to membrane curvature. Their self-assembly then further drives membrane remodeling to create plasma membrane invaginations (caveolins) or tubulate the endoplasmic reticulum (reticulons). By combining a wedge-shaped hydrophobic structure with oligomerization, these proteins can induce significant local curvature without occupying a large amount of the membrane surface. Thus, they are effective curvature generators that are compatible with recruitment of effectors for receptor signaling and other functions<sup>44</sup>.

## Self-assembling soluble coat scaffolds

Moving outward from the membrane surface, membrane binding adaptor proteins frequently recruit coats to the membrane surface. Perhaps the best-characterized examples of protein assembly driving membrane curvature are two of the canonical coats, clathrin and COPII. Both coats contain elements that polymerize into polyhedral structures independent of membranes<sup>45</sup>. As noted, the favorable energetics of clathrin or COPII assembly alone can induce vesicle formation without membrane-inserted motifs<sup>32,27</sup>. However, the structure

formed by the COPII outer coat scaffold does not employ the significant intertwining that occurs during clathrin triskelion assembly, relying instead on less extensive interactions among coat protomers. Thus, the energy derived from assembly of COPII interfaces is likely less than that derived from clathrin assembly. In the case of the COPI coat, self-assembly into a cage-like structure has not been observed, and electron microscopy of liposome-derived COPI vesicles reveals both gaps in coat packing and alternative packing interactions on vesicles of different size<sup>46</sup>, suggesting a more labile scaffold. Adaptor recruitment alone could also contribute to membrane bending (Figure 2D), especially if additional organization promotes steric pressure. The plastic COPI coat could contribute to membrane bending through this mechanism, as well as by forming a rigid scaffold. AP3-mediated sorting events, which can occur without clathrin, may rely on Vps41 as a self-assembling element<sup>47</sup>, but whether this assembly provides a bona fide scaffold or promotes adaptor aggregation remains to be established. In the case of the two COP coats, membrane recruitment is mediated by small GTPases with amphipathic helices. As described above, it is not completely clear whether these contribute to bending by inserting in the cytoplasmic leaflet<sup>27,48</sup> or serve as lipid-interactors that alter membrane rigidity<sup>33</sup> or both. Clathrin assembly at the TGN and endosome employs ARF1<sup>49</sup> and ARF6<sup>50</sup> respectively. The use of these accessories may reflect different bending challenges at the different cellular locations.

Although no experimentally determined numbers exist for the free energy generated by clathrin or COP scaffold assembly at membranes, it is clear that the individual interactions of scaffold components are of sufficiently low affinity to be reversible<sup>51</sup>. Experimental evidence that clathrin assembly can directly vesiculate membranes<sup>32</sup>, is consistent with higher estimates of clathrin-clathrin interactions<sup>7,52</sup> rather than lower estimates<sup>53</sup>. Further, cellular clathrin depolymerization (uncoating) clearly requires ATP-hydrolysis by HSP70 stimulated by the DNAJ-homolog auxilin/Swa2, in a process that requires direct interaction with the coat protein<sup>49</sup>. COPI and COPII coat disassembly, on the other hand, is modulated by their anchoring small GTPases and they apparently disassemble spontaneously following GTP hydrolysis<sup>34,54</sup>. One outstanding question is whether the energy invested in vesicle formation is sufficient to force curvature of membranes such that the closed vesicle released from the donor membrane remains under curvature stress. We speculate that such accumulated tension might “prime” a vesicle for fusion such that the stored energy will promote SNARE-mediated fusion events when the vesicle docks with the target membrane. In this model, the energy invested in forming a highly curved vesicle could help to pay the energetic cost of membrane fusion, providing a role for curvature drivers in both vesicle biogenesis and consumption.

A final important physical parameter associated with coat scaffolds with direct relevance to membrane bending is the need for rigidity, which presumably translates into stronger bending forces and is seemingly required to enforce curvature on certain cargo-containing membranes. For example, structural modeling suggests that the outer COPII coat protein, Sec13, acts to rigidify the coat such that it can enforce curvature on wild-type membranes. In yeast, Sec13 becomes dispensable when traffic of GPI-anchored cargoes is diminished, linking coat rigidity to a specific cargo burden<sup>15</sup>. In support of this model, knockdown of mammalian Sec13 has minimal impact on bulk protein secretion but impedes ER export of collagen<sup>55</sup>, which might contribute a significant barrier to curvature by virtue of its polymeric state<sup>56</sup>. Similarly, the clathrin light chain subunit, which confers rigidity on the proximal leg of the triskelion, is dispensable for receptor-mediated endocytosis of transferrin and epidermal growth factor receptor<sup>57</sup>. However, some G protein-coupled receptors require the presence of clathrin light chains for their uptake<sup>58</sup>. While this was suggested to be an effect on clathrin uncoating, it might also reflect a need for greater rigidity of coats that must internalize GPCR plus their associated arrestin and signaling subunit baggage.

## Actin polymerization

Beyond membrane cargo and membrane-associated adaptors and coats, the actin cytoskeleton frequently plays an indispensable role in membrane curvature. In some cellular circumstances, membrane deformation by the mechanisms described above is not sufficient to induce vesicle budding. In these cases, actin polymerization is coordinated with membrane-bending proteins to generate the force required for budding. Actin can play three roles in budding. One role is to help the vesicle pinching process by polymerization at the neck of a budding vesicle, pushing the vesicle away from the membrane and/or providing constricting force. For clathrin-coated vesicles forming in yeast, actin is constitutively needed at the neck of a budding coated vesicle to overcome turgor pressure on the membrane<sup>6</sup>. Indeed, the effect of turgor, combined with the small size of yeast endocytic vesicles, may form such a strong barrier to curvature that membrane bending isn't detected until actin polymerization occurs<sup>59</sup>. Similarly, in mammalian cell membranes under tension, either induced by the presence of microvilli on apical membranes or by artificially generated tension, actin polymerization is required for budding<sup>7</sup>. These clathrin-associated actin pathways involve the connection between the clathrin light chain subunits and Hip proteins<sup>49</sup>. Interestingly, electron microscopy analysis of mammalian cells<sup>60</sup> reveals actin at the neck of most endocytic clathrin-coated vesicles, indicating that most plasma membrane budding uses actin. In this feature, mammalian endocytic clathrin-coated vesicles resemble yeast endocytic clathrin-coated vesicles<sup>61</sup>, though the former has variable requirements for actin, while the latter has absolute requirements. Despite these findings on the important role of actin in membrane bending and endocytosis, it has also been shown that depolymerization of the actin cytoskeleton does not significantly inhibit clathrin-mediated endocytosis in multiple cell types<sup>62</sup>.

Another mechanism by which actin contributes to endocytosis relies on actin's ability to extend membrane protrusions by polymerization and induce localized phagocytosis. When clathrin coats are flat and cargo is too large to be surrounded by a scaffold, actin operates to cause endocytosis. This is observed during uptake of clathrin plaques<sup>63</sup>, uptake of bacteria where clathrin serves as an actin-assembly nucleator<sup>64</sup> and with viral particles that are too large to fit in conventional clathrin-coated pits<sup>65</sup>. Uptake of virus by endocytosis in caveolae works by a similar principle and requires actin<sup>66</sup>. A third role for actin, which is less established, may be to contribute to vesicle biogenesis from tubules<sup>67</sup>. Yeast TGN-derived vesicles travel on actin cables to polarized sites of growth and thus may also employ actin in their biogenesis. Directed endosomal recycling in mammalian cells also involves actin-organizing proteins, particularly during cell migration, which could play a role in generating recycling vesicles<sup>68</sup>.

Once these drivers have acted to generate nascent vesicle buds, additional membrane remodeling occurs during vesicle release. Pinching at the neck of a vesicle is a special case of extreme membrane bending to promote fusion, and involves complex curvature that seems to require specialized protein machines<sup>69</sup>. In metazoan cells, force for this process is exerted by self-assembly of dynamin into collars, which can also recruit actin<sup>70</sup>. Additional influence can come from BAR-domain containing proteins that oligomerize to scaffold membrane curvature. In the case of dynamins<sup>71</sup> and BAR-domain proteins<sup>72</sup>, membrane insertion events might make an important contribution by virtue of the high surface density of these oligomeric proteins.

## An accounting of the energetic forces that drive and oppose membrane curvature

We have discussed the various mechanisms by which lipids, membrane-bound proteins, self-assembling scaffolds and actin contribute to membrane bending during vesicle formation. In the cell, multiple components deploy these mechanisms in a complementary and cooperative fashion. Here we provide an accounting of the energetics involved in membrane bending, using the clathrin system as a model, based on previously published calculations of the contributions of the components we have described (see Box 1). In doing so, we aim to approximate the relative contributions of each component to vesicle formation and to investigate whether our current understanding of the physical forces underlying membrane bending is sufficient to explain vesicle formation. This approach does not incorporate the entire spectrum of physical effects, especially those driven by accessory proteins, largely because these effects have not yet been precisely quantified. Further, since the number of independently published quantitative estimates of the individual bending effects is still quite small, we expect these estimates to be revised repeatedly over the next few years. In particular, the contribution of actin to vesicle formation is based on a single, very recent estimate<sup>7</sup>. Nonetheless, we consider that this quantitative approach provides a valuable illustration of the problem of the cost-driver balance of forming highly curved vesicles from cellular membranes.

Returning first to the Canham and Helfrich models of membrane bending<sup>4,5</sup>, we can calculate the energetic cost of bending a piece of initially flat membrane into a spherical vesicle by understanding the bending rigidity. This force, expressed in units of energy, ranges from  $10k_B T$  for highly fluid membranes composed entirely of lipids with unsaturated tails<sup>73</sup> to approximately  $50k_B T$  for fluid membranes containing 50% cholesterol<sup>74</sup>, similar in composition to the plasma membrane of mammalian cells<sup>75</sup>, where  $k_B$  is Boltzmann's constant and  $T$  is temperature (Figure 3A; Box 1). The energetic barrier to membrane stretching is the product of membrane tension and membrane surface area. Membrane tension arises from thermal fluctuations within the membrane<sup>74</sup>, osmotic imbalances across the membrane and application of forces to the membrane by the cytoskeleton in cellular structures such as villi<sup>7</sup>, and by a cell wall. Physiological values of membrane tension are in the range of  $0.2-1 \times 10^3 k_B T/nm^2$ <sup>76</sup>. For a typical vesicle of 100 nm diameter, the energetic cost per membrane area of overcoming membrane tension is therefore 10-100 times smaller than the energetic cost per membrane area of membrane bending ( $8-40 \times 10^{-3} k_B T/nm^2$ ) such that membrane bending is usually cited as the most significant lipid-associated barrier to deforming membranes.

The energetic costs of cargo crowding are more difficult to model, being somewhat dependent on the specific protein composition of the underlying membrane, with asymmetrically distributed and lumenally oriented proteins having a larger effect than those that are symmetrically proportioned. However, a recently published model has estimated the energetic costs of the entropic effects of membrane-attached proteins as a function of the size and density of proteins bound to membrane surfaces<sup>31</sup>. Applying these results to two hypothetical vesicle budding scenarios that contain either asymmetrically or symmetrically distributed cargo proteins (Figure 3B) suggests that both orientations contribute a significant barrier, especially as the diameter of the vesicle decreases. It is initially surprising that symmetric cargo proteins oppose curvature nearly as strongly as highly asymmetric ones. This behavior is a consequence of the highly non-linear increase in steric pressure with protein density. Owing to this nonlinearity, crowding effects are much stronger on the inner leaflet of a small vesicle than on the outer leaflet. Therefore, crowding on the outer leaflet by symmetric cargos only slightly reduces the barrier to membrane bending.



Turning to the drivers of curvature and compiling recent estimates from the literature (Figure 3C), we find that the effect of hydrophobic insertions is relatively small, where one insertion was included for each adaptor protein with a stoichiometry of approximately two adaptor proteins per clathrin triskelion (see Box 1 for detailed analysis). Since insertions contribute to membrane bending on a per area basis, their energetic contribution per membrane area remains constant across vesicles of different sizes. Crowding effects of the cargo-bound adaptor complexes contribute significantly, with a larger impact as vesicle diameter decreases. Clathrin and actin polymerization are both significant contributors that make a fixed contribution per membrane area. These estimates represent data from diverse experiments that likely be refined and revised by future work. Therefore, their interpretation at this stage must remain largely qualitative. Nonetheless, from combining these findings, it appears that the energetic costs (bending rigidity and tension<sup>4,5,73,74</sup>, cargo crowding<sup>15,31</sup>) of producing vesicles of moderate size (~50nm diameter) is offset by the energetic drivers when all drivers are present (coat polymerization<sup>52</sup>, accessory protein crowding<sup>31</sup>, amphipathic insertion<sup>26,30</sup>, cytoskeletal forces<sup>60,77</sup>), whereas producing smaller vesicles and vesicle production in the absence of one or more drivers cannot be fully accounted for (Figure 3D). Synaptic vesicles represent an extreme example of a highly curved vesicle, measuring just 40nm in diameter. Formation of these vesicles is independent of actin<sup>78</sup> and thus would seem to be energetically unfavorable in our analysis (Figure 3D). However, detailed structural and proteomic analysis of synaptic vesicles reveals that a large number of the embedded protein cargoes are cytoplasmically oriented and thus may contribute positively to membrane bending rather than acting as a barrier. In this example, the energetic cost of membrane bending would be overestimated and cargo itself could be considered as a driver. Indeed, the detailed molecular map of synaptic vesicles<sup>10</sup> serves as a benchmark that other vesicle systems might aspire to in order to fully appreciate the underlying costs and drivers of an individual budding event. In sum, our analysis demonstrates that different properties of cellular membranes engender distinct requirements in terms of the energetics of coat scaffold assembly, the role of actin and the need for additional accessory factors like BAR-domains and dynamin that can provide additional curvature and/or force.

Ultimately, cellular membrane curvature involves the coordination of multiple complementary and cooperative mechanisms. Such coordination has been elegantly demonstrated for clathrin-coated pit formation by single molecule imaging. Cooperative interactions between cargo-bound adaptors recruited scaffold-forming coat molecules that in turn attracted other membrane benders<sup>79</sup>. Intracellular pathogens provide further examples of diverse solutions to the membrane bending problem. The outer coat of trypanosomes is formed by GPI-anchored proteins that might create bending challenges through leaflet asymmetry and cargo crowding. Notably, these organisms alter the packing of their surface proteins by glycosylation that could reduce crowding or rigidity<sup>80</sup>. In another pathogenic example, clathrin is implicated in organizing retroviral glycoproteins during viral budding, which might induce crowding that enforces external budding<sup>81</sup>. This may be comparable to crowding effects of Herpes virus capsid proteins, which may have a positive influence on budding<sup>82</sup>. In conclusion, the simple principles of membrane bending that we have discussed here can be orchestrated in a variety of combinations to mediate membrane budding in biological membranes both for normal cellular function and during pathogenesis.

## Acknowledgments

JCS acknowledges funding from the UT Austin Cockrell School of Engineering and the Texas 4000 Cancer Seed Grant Program. FMB and EAM acknowledge support from the National Institute of General Medical Science of the National Institutes of Health under award numbers R01GM038093 (FMB), R01GM078186 (EAM) and R01GM085089 (EAM). We thank Dr. M.C.S. Lee (Columbia University), Dr. E. Schmid (UC Berkeley), Dr. C.

Hayden (Sandia Labs) and Dr. E. Lafer (UT Health Science Center) for thoughtful discussions and comments on the manuscript.

## References

1. McMahon HT, Gallop JL. Membrane curvature and mechanisms of dynamic cell membrane remodelling. *Nature*. 2005; 438:590–6. [PubMed: 16319878]
2. Bigay J, Antonny B. Curvature, lipid packing, and electrostatics of membrane organelles: defining cellular territories in determining specificity. *Dev Cell*. 2012; 23:886–95. [PubMed: 23153485]
3. Zimmerberg J, Kozlov MM. How proteins produce cellular membrane curvature. *Nat Rev Mol Cell Biol*. 2006; 7:9–19. [PubMed: 16365634]
4. Canham PB. The minimum energy of bending as a possible explanation of the biconcave shape of the human red blood cell. *Journal of theoretical biology*. 1970; 26:61–81. [PubMed: 5411112]
5. Helfrich W. Elastic properties of lipid bilayers: theory and possible experiments. *Zeitschrift fur Naturforschung Teil C: Biochemie, Biophysik, Biologie, Virologie*. 1973; 28:693–703.
6. Aghamohammadzadeh S, Ayscough KR. Differential requirements for actin during yeast and mammalian endocytosis. *Nature Cell Biology*. 2009; 11:1039–42.
7. Boulant S, Kural C, Zeeh JC, Ubelmann F, Kirchhausen T. Actin dynamics counteract membrane tension during clathrin-mediated endocytosis. *Nature Cell Biology*. 2011; 13:1124–31.
8. Svetina S, Zeks B. Membrane bending energy and shape determination of phospholipid vesicles and red blood cells. *European biophysics journal: EBJ*. 1989; 17:101–11. [PubMed: 2766997]
9. Fuller N, Rand RP. The influence of lysolipids on the spontaneous curvature and bending elasticity of phospholipid membranes. *Biophysical Journal*. 2001; 81:243–54. [PubMed: 11423410]
10. Takamori S, et al. Molecular anatomy of a trafficking organelle. *Cell*. 2006; 127:831–46. [PubMed: 17110340]
11. Fujita M, Kinoshita T. GPI-anchor remodeling: potential functions of GPI-anchors in intracellular trafficking and membrane dynamics. *Biochim Biophys Acta*. 2012; 1821:1050–8. [PubMed: 22265715]
12. Sheetz MP, Singer SJ. Biological membranes as bilayer couples, A molecular mechanism of drug-erythrocyte interactions. *Proceedings of the National Academy of the Sciences of the United States of America*. 1974; 71:4457–4461.
13. Decher G, et al. Interaction of Amphiphilic Polymers with Model Membranes. *Angewandte Makromolekulare Chemie*. 1989; 166:71–80.
14. Stachowiak JC, Hayden CC, Sasaki DY. Steric confinement of proteins on lipid membranes can drive curvature and tubulation. *Proc Natl Acad Sci U S A*. 2010; 107:7781–6. [PubMed: 20385839]
15. Copic A, Latham CF, Horlbeck MA, D’Arcangelo JG, Miller EA. ER Cargo Properties Specify a Requirement for COPII Coat Rigidity Mediated by Sec13p. *Science*. 2012
16. Sharpe HJ, Stevens TJ, Munro S. A comprehensive comparison of transmembrane domains reveals organelle-specific properties. *Cell*. 2010; 142:158–69. [PubMed: 20603021]
17. Roth TF, Porter KR. Yolk Protein Uptake in the Oocyte of the Mosquito *Aedes Aegypti*. *J Cell Biol*. 1964; 20:313–32. [PubMed: 14126875]
18. Pearse BM, Crowther RA. Structure and assembly of coated vesicles. *Annu Rev Biophys Biophys Chem*. 1987; 16:49–68. [PubMed: 2885011]
19. Thomas PD, Poznansky MJ. Curvature and Composition-Dependent Lipid Asymmetry in Phosphatidylcholine Vesicles Containing Phosphatidylethanolamine and Gangliosides. *Biochimica Et Biophysica Acta*. 1989; 978:85–90. [PubMed: 2914133]
20. Goni FM, Alonso A. Biophysics of sphingolipids I. Membrane properties of sphingosine, ceramides and other simple sphingolipids. *Biochimica et biophysica acta*. 2006; 1758:1902–21. [PubMed: 17070498]
21. Hailey DW, et al. Mitochondria Supply Membranes for Autophagosome Biogenesis during Starvation. *Cell*. 2010; 141:656–667. [PubMed: 20478256]
22. Yang JS, et al. A role for phosphatidic acid in COPI vesicle fission yields insights into Golgi maintenance. *Nat Cell Biol*. 2008; 10:1146–53. [PubMed: 18776900]

23. Gall WE, et al. Drs2p-dependent formation of exocytic clathrin-coated vesicles in vivo. *Curr Biol*. 2002; 12:1623–7. [PubMed: 12372257]
24. Zha X, et al. Sphingomyelinase treatment induces ATP-independent endocytosis. *J Cell Biol*. 1998; 140:39–47. [PubMed: 9425152]
25. Leibler S. Curvature instability in membranes. *J Phys*. 1986; 47:507–516.
26. Ford MG, et al. Curvature of clathrin-coated pits driven by epsin. *Nature*. 2002; 419:361–6. [PubMed: 12353027]
27. Lee MCS, et al. Sar1p N-terminal helix initiates membrane curvature and completes the fission of a COPII vesicle. *Cell*. 2005; 122:605–17. [PubMed: 16122427]
28. Lundmark R, Doherty GJ, Vallis Y, Peter BJ, McMahon HT. Arf family GTP loading is activated by, and generates, positive membrane curvature. *Biochem J*. 2008; 414:189–94. [PubMed: 18597672]
29. Krauss M, et al. Arf1-GTP-induced tubule formation suggests a function of Arf family proteins in curvature acquisition at sites of vesicle budding. *J Biol Chem*. 2008; 283:27717–23. [PubMed: 18693248]
30. Campelo F, McMahon HT, Kozlov MM. The hydrophobic insertion mechanism of membrane curvature generation by proteins. *Biophys J*. 2008; 95:2325–39. [PubMed: 18515373]
31. Stachowiak JC, et al. Membrane bending by protein-protein crowding. *Nature Cell Biology*. 2012; 14:944–9.
32. Dannhauser PN, Ungewickell EJ. Reconstitution of clathrin-coated bud and vesicle formation with minimal components. *Nat Cell Biol*. 2012; 14:634–9. [PubMed: 22522172]
33. Settles EI, Loftus AF, McKeown AN, Parthasarathy R. The vesicle trafficking protein Sar1 lowers lipid membrane rigidity. *Biophys J*. 2010; 99:1539–45. [PubMed: 20816066]
34. Bigay J, Gounon P, Robineau S, Antonny B. Lipid packing sensed by ArfGAP1 couples COPI coat disassembly to membrane bilayer curvature. *Nature*. 2003; 426:563–6. [PubMed: 14654841]
35. Tsafirir I, Caspi Y, Guedeau-Boudeville MA, Arzi T, Stavans J. Budding and tubulation in highly oblate vesicles by anchored amphiphilic molecules. *Phys Rev Lett*. 2003; 91:138102. [PubMed: 14525338]
36. Lipowsky R. Bending of Membranes by Anchored Polymers. *Europhysics Letters*. 1995; 30:197–202.
37. Kim YW, Sung WY. Membrane curvature induced by polymer adsorption. *Physical Review E*. 2001:63.
38. Imjeti NS, et al. N-Glycosylation instead of cholesterol mediates oligomerization and apical sorting of GPI-APs in FRT cells. *Mol Biol Cell*. 2011; 22:4621–34. [PubMed: 21998201]
39. Tooze SA, Martens GJ, Huttner WB. Secretory granule biogenesis: rafting to the SNARE. *Trends Cell Biol*. 2001; 11:116–22. [PubMed: 11306272]
40. Vennema H, et al. Nucleocapsid-independent assembly of coronavirus-like particles by co-expression of viral envelope protein genes. *The EMBO journal*. 1996; 15:2020–8. [PubMed: 8617249]
41. Wang CW, Hamamoto S, Orci L, Schekman R. Exomer: A coat complex for transport of select membrane proteins from the trans-Golgi network to the plasma membrane in yeast. *J Cell Biol*. 2006; 174:973–83. [PubMed: 17000877]
42. Shibata Y, et al. The reticulon and DP1/Yop1p proteins form immobile oligomers in the tubular endoplasmic reticulum. *J Biol Chem*. 2008; 283:18892–904. [PubMed: 18442980]
43. Walser PJ, et al. Constitutive formation of caveolae in a bacterium. *Cell*. 2012; 150:752–63. [PubMed: 22901807]
44. Hu J, et al. Membrane proteins of the endoplasmic reticulum induce high-curvature tubules. *Science*. 2008; 319:1247–50. [PubMed: 18309084]
45. Stagg SM, et al. Structure of the Sec13/31 COPII coat cage. *Nature*. 2006; 439:234–8. [PubMed: 16407955]
46. Faini M, et al. The structures of COPI-coated vesicles reveal alternate coatomer conformations and interactions. *Science*. 2012; 336:1451–4. [PubMed: 22628556]

47. Darsow T, Katzmann DJ, Cowles CR, Emr SD. Vps41p function in the alkaline phosphatase pathway requires homo-oligomerization and interaction with AP-3 through two distinct domains. *Mol Biol Cell*. 2001; 12:37–51. [PubMed: 11160821]
48. Bielli A, et al. Regulation of Sar1 NH2 terminus by GTP binding and hydrolysis promotes membrane deformation to control COPII vesicle fission. *J Cell Biol*. 2005; 171:919–24. [PubMed: 16344311]
49. Brodsky FM. Diversity of clathrin function: new tricks for an old protein. *Annu Rev Cell Dev Biol*. 2012; 28:309–36. [PubMed: 22831640]
50. Luo Y, Zhan Y, Keen JH. Arf6 Regulation of Gyating-Clathrin. *Traffic*. 2012
51. Wakeham DE, Chen CY, Greene B, Hwang PK, Brodsky FM. Clathrin self-assembly involves coordinated weak interactions favorable for cellular regulation. *EMBO J*. 2003; 22:4980–90. [PubMed: 14517237]
52. den Otter WK, Briels WJ. The generation of curved clathrin coats from flat plaques. *Traffic*. 2011; 12:1407–16. [PubMed: 21718403]
53. Nossal R. Energetics of clathrin basket assembly. *Traffic*. 2001; 2:138–47. [PubMed: 11247304]
54. Antonny B, Madden D, Hamamoto S, Orci L, Schekman R. Dynamics of the COPII coat with GTP and stable analogues. *Nat Cell Biol*. 2001; 3:531–7. [PubMed: 11389436]
55. Townley AK, et al. Efficient coupling of Sec23-Sec24 to Sec13-Sec31 drives COPII-dependent collagen secretion and is essential for normal craniofacial development. *J Cell Sci*. 2008; 121:3025–34. [PubMed: 18713835]
56. Malhotra V, Erlmann P. Protein export at the ER: loading big collagens into COPII carriers. *EMBO J*. 2011; 30:3475–80. [PubMed: 21878990]
57. Huang F, Sorkin A. Growth factor receptor binding protein 2-mediated recruitment of the RING domain of Cbl to the epidermal growth factor receptor is essential and sufficient to support receptor endocytosis. *Mol Biol Cell*. 2005; 16:1268–81. [PubMed: 15635092]
58. Ferreira F, et al. Endocytosis of G protein-coupled receptors is regulated by clathrin light chain phosphorylation. *Curr Biol*. 2012; 22:1361–70. [PubMed: 22704991]
59. Kukulski W, Schorb M, Kaksonen M, Briggs JAG. Plasma Membrane Reshaping during Endocytosis Is Revealed by Time-Resolved Electron Tomography. *Cell*. 2012; 150:508–520. [PubMed: 22863005]
60. Collins A, Warrington A, Taylor KA, Svitkina T. Structural organization of the actin cytoskeleton at sites of clathrin-mediated endocytosis. *Current biology: CB*. 2011; 21:1167–75. [PubMed: 21723126]
61. Idrissi FZ, Blasco A, Espinal A, Geli MI. Ultrastructural dynamics of proteins involved in endocytic budding. *Proc Natl Acad Sci USA*. 2012; 109:E2587–94. [PubMed: 22949647]
62. Fujimoto LM, Roth R, Heuser JE, Schmid SL. Actin assembly plays a variable, but not obligatory role in receptor-mediated endocytosis in mammalian cells. *Traffic*. 2000; 1:161–71. [PubMed: 11208096]
63. Saffarian S, Cocucci E, Kirchhausen T. Distinct dynamics of endocytic clathrin-coated pits and coated plaques. *PLoS Biol*. 2009; 7:e1000191. [PubMed: 19809571]
64. Bonazzi M, et al. Clathrin phosphorylation is required for actin recruitment at sites of bacterial adhesion and internalization. *J Cell Biol*. 2011; 195:525–36. [PubMed: 22042622]
65. Cureton DK, Massol RH, Whelan SP, Kirchhausen T. The length of vesicular stomatitis virus particles dictates a need for actin assembly during clathrin-dependent endocytosis. *PLoS Pathog*. 2010; 6:e1001127. [PubMed: 20941355]
66. Hansen CG, Nichols BJ. Exploring the caves: cavins, caveolins and caveolae. *Trends Cell Biol*. 2010; 20:177–86. [PubMed: 20153650]
67. Karpova TS, et al. Role of actin and Myo2p in polarized secretion and growth of *Saccharomyces cerevisiae*. *Mol Biol Cell*. 2000; 11:1727–37. [PubMed: 10793147]
68. Zech T, Calaminus SD, Machesky LM. Actin on trafficking: Could actin guide directed receptor transport? *Cell Adh Migr*. 2012; 6:476–81. [PubMed: 23076144]
69. Campelo F, Malhotra V. Membrane fission: the biogenesis of transport carriers. *Annu Rev Biochem*. 2012; 81:407–27. [PubMed: 22463692]

70. Ferguson SM, De Camilli P. Dynamin, a membrane-remodelling GTPase. *Nat Rev Mol Cell Biol.* 2012; 13:75–88. [PubMed: 22233676]
71. Schmid SL, Frolov VA. Dynamin: functional design of a membrane fission catalyst. *Annu Rev Cell Dev Biol.* 2011; 27:79–105. [PubMed: 21599493]
72. Boucrot E, et al. Membrane fission is promoted by insertion of amphipathic helices and is restricted by crescent BAR domains. *Cell.* 2012; 149:124–36. [PubMed: 22464325]
73. Rawicz W, Olbrich KC, McIntosh T, Needham D, Evans E. Effect of chain length and unsaturation on elasticity of lipid bilayers. *Biophysical Journal.* 2000; 79:328–39. [PubMed: 10866959]
74. Evans E, Rawicz W. Entropy-Driven Tension and Bending Elasticity in Condensed-Fluid Membranes. *Physical Review Letters.* 1990; 64:2094–2097. [PubMed: 10041575]
75. van Meer G, Voelker DR, Feigenson GW. Membrane lipids: where they are and how they behave. *Nat Rev Mol Cell Biol.* 2008; 9:112–24. [PubMed: 18216768]
76. Hochmuth FM, Shao JY, Dai J, Sheetz MP. Deformation and flow of membrane into tethers extracted from neuronal growth cones. *Biophysical journal.* 1996; 70:358–69. [PubMed: 8770212]
77. Liu J, Kaksonen M, Drubin DG, Oster G. Endocytic vesicle scission by lipid phase boundary forces. *Proceedings of the National Academy of Sciences of the United States of America.* 2006; 103:10277–82. [PubMed: 16801551]
78. Sankaranarayanan S, Atluri PP, Ryan TA. Actin has a molecular scaffolding, not propulsive, role in presynaptic function. *Nat Neurosci.* 2003; 6:127–35. [PubMed: 12536209]
79. Cocucci E, Aguet F, Boulant S, Kirchhausen T. The first five seconds in the life of a clathrin-coated pit. *Cell.* 2012; 150:495–507. [PubMed: 22863004]
80. Mehlert A, Wormald MR, Ferguson MA. Modeling of the N-glycosylated transferrin receptor suggests how transferrin binding can occur within the surface coat of *Trypanosoma brucei*. *PLoS Pathog.* 2012; 8:e1002618. [PubMed: 22496646]
81. Zhang F, Zang T, Wilson SJ, Johnson MC, Bieniasz PD. Clathrin facilitates the morphogenesis of retrovirus particles. *PLoS Pathog.* 2011; 7:e1002119. [PubMed: 21738476]
82. Johnson DC, Baines JD. Herpesviruses remodel host membranes for virus egress. *Nat Rev Microbiol.* 2011; 9:382–94. [PubMed: 21494278]
83. Fotin A, et al. Molecular model for a complete clathrin lattice from electron cryomicroscopy. *Nature.* 2004; 432:573–9. [PubMed: 15502812]
84. Hierro A, et al. Functional architecture of the retromer cargo-recognition complex. *Nature.* 2007; 449:1063–7. [PubMed: 17891154]
85. Tanaka-Takiguchi Y, Kinoshita M, Takiguchi K. Septin-mediated uniform bracing of phospholipid membranes. *Curr Biol.* 2009; 19:140–5. [PubMed: 19167227]
86. Effantin G, et al. ESCRT-III CHMP2A and CHMP3 form variable helical polymers in vitro and act synergistically during HIV-1 budding. *Cell Microbiol.* 2013; 15:213–26. [PubMed: 23051622]
87. Carnahan NF, Starling KE. Equation of State for Nonattracting Rigid Spheres. *Journal of Chemical Physics.* 1969; 51:635.
88. Song YH, Mason EA, Stratt RM. Why Does the Carnahan-Starling Equation Work So Well. *Journal of Physical Chemistry.* 1989; 93:6916–6919.
89. Scheve CS, Gonzales PA, Momin N, Stachowiak JC. Steric Pressure between Membrane-Bound Proteins Opposes Lipid Phase Separation. *Journal of the American Chemical Society.* 2013; 135:1185–1188. [PubMed: 23321000]
90. Blondeau F, et al. Tandem MS analysis of brain clathrin-coated vesicles reveals their critical involvement in synaptic vesicle recycling. *Proc Natl Acad Sci U S A.* 2004; 101:3833–8. [PubMed: 15007177]

**Box 1****Calculations and assumptions of approximate energetic analysis for formation of coated vesicles**

All energetic costs and drivers were estimated in terms of energy per membrane area (units of  $k_B T/\text{nm}^2$ ) as a function of coated vesicle diameter for a range of 25-100 nm.

**Energetic Costs of Forming Coated Vesicles**

1. *Membrane bending:* Using the classic Canham, Helfrich, and Evans theory<sup>4,5</sup>, the energetic cost per membrane area of creating a curved sphere was estimated as  $G_{bending} = (8\kappa)/(4r^2)$ , where  $\kappa$  is the bending rigidity of the membrane, and  $r$  is the vesicle radius. Calculations were performed for soft fluid membranes for which  $\kappa \sim 10k_B T$  and for membranes containing 50% cholesterol (typical value for mammalian plasma membrane), for which  $\kappa \sim 50k_B T$ <sup>74</sup>.
2. *Membrane tension:* The finite tension of biological membranes opposes changes in shape. The membrane tension, which has units of energy per area, is approximately the energy required per membrane area to form a spherical vesicle from the membrane surface. A typical value of  $0.02 k_B T/\text{nm}^2$  was estimated, based on micropipette aspiration measurements of membrane tension before significant straining<sup>74</sup>.
3. *Cargo crowding:* When an initially flat region of the membrane becomes curved, the luminal domains of cargo molecules have less space to diffuse on the membrane surface, owing to the negative curvature of the vesicle inner surface. The reduced entropy of cargo molecules leads to an increased pressure on the membrane surface that can be expressed as an energetic cost per membrane area. Conversely, cargo molecules that have a domain on the coat side of the membrane will experience a reduction in steric congestion, an energetic contribution that encourages membrane curvature. The difference between these terms is the approximate energetic cost of cargo crowding. The net energetic cost per membrane area of crowding was calculated by assuming a cargo molecule with either (i) a single luminal domain of 5 nm diameter (asymmetric case) or (ii) domains of 5 nm diameter on both sides of the membrane (symmetric case), where luminal domains cover 50% of the initially flat membrane surface area<sup>16</sup>. Surface pressures on both membrane surfaces were estimated using a non-linear equation of state for hard discs in two dimensions as proposed by Carnahan and Starling<sup>87,88</sup> and used recently to estimate the surface pressure due to protein crowding on membrane surfaces<sup>31,89</sup>.

**Energetic Drivers for Forming Coated Vesicles**

1. *Clathrin polymerization:* Coarse-grained molecular simulations by den Otter et al. have recently estimated that  $25 k_B T$  is released per clathrin triskelia when a clathrin lattice assembles.<sup>52</sup> Dividing this value by the membrane surface area occupied per triskelia of a lattice ( $\sim 300 \text{ nm}^2$ , Fotin et al.<sup>83</sup>), the energetic contribution of clathrin assembly per membrane area was estimated as approximately  $0.08 k_B T/\text{nm}^2$ .
2. *Accessory protein (AP) Crowding:* When an initially flat portion of the membrane surfaces curves to form a clathrin-coated vesicle, accessory proteins beneath the clathrin lattice are able to explore a larger region of the membrane surface, owing to the positive curvature of the outer vesicle surface. This increased entropy decreases the membrane surface pressure, which can be described as a reduction in free energy per membrane area. Assuming that 75%

of the membrane surface is occupied by accessory proteins<sup>90</sup> and that an average AP has a diameter of 5-10 nm, the energetic contribution of AP crowding was estimated using the same approach used to estimate the cost of cargo crowding.

3. *Actin polymerization:* A dense collar of actin filaments surrounds clathrin-coated vesicles, contributing to vesicle formation<sup>60</sup>. Recent studies have suggested that polymerization of these filaments does work that helps clathrin-coated vesicles to form<sup>7,59</sup>. The energetic contribution of actin polymerization to vesicle budding must vary with the density and geometrical arrangement of filaments, parameters which are still being defined and likely differ from one physiological situation to another. Here we include an energetic contribution of  $0.13 \text{ k}_B\text{T}/\text{nm}^2$ , based on the recent report that osmotic swelling of mammalian cells creates a requirement for actin to efficiently complete clathrin-mediated endocytosis<sup>7</sup>. In this report, the work,  $W$ , required to form a vesicle against membrane tension,  $\sigma$ , was estimated as  $W = 4\pi r^2 \sigma$ . Roughly estimating the elevated membrane tension to be approximately half the lytic limit ( $\sim 0.5 \text{ k}_B\text{T}/\text{nm}^2$ <sup>74</sup>), and dividing the work,  $W$ , by the vesicle surface area ( $4\pi r^2$ ), we estimate the contribution of actin required to overcome high membrane tension as approximately  $0.13 \text{ k}_B\text{T}/\text{nm}^2$ .
4. *Hydrophobia Insertion:* Clathrin assembly proteins, such as Epsin1 insert amphipathic helices when they bind to membrane surface<sup>26</sup>. The energetic contribution of helix insertion was taken from Campelo et al.<sup>30</sup> assuming that a maximum of 2% of the membrane surface area is covered by insertions. Under this condition, Campelo et al. predicts a membrane radius of curvature of about 130 nm. Using the expression,  $G_{bending} = (8\pi\kappa)/(4\pi r^2)$ , to calculate the bending energy and assuming a bending rigidity of  $50 \text{ k}_B\text{T}$ , we arrive at a value of  $0.006 \text{ k}_B\text{T}/\text{nm}^2$  for insertions. The 2% insertion area is the maximum expected if each adaptor protein provides an insertion and occupies  $50 \text{ nm}^2$  on the membrane surface.

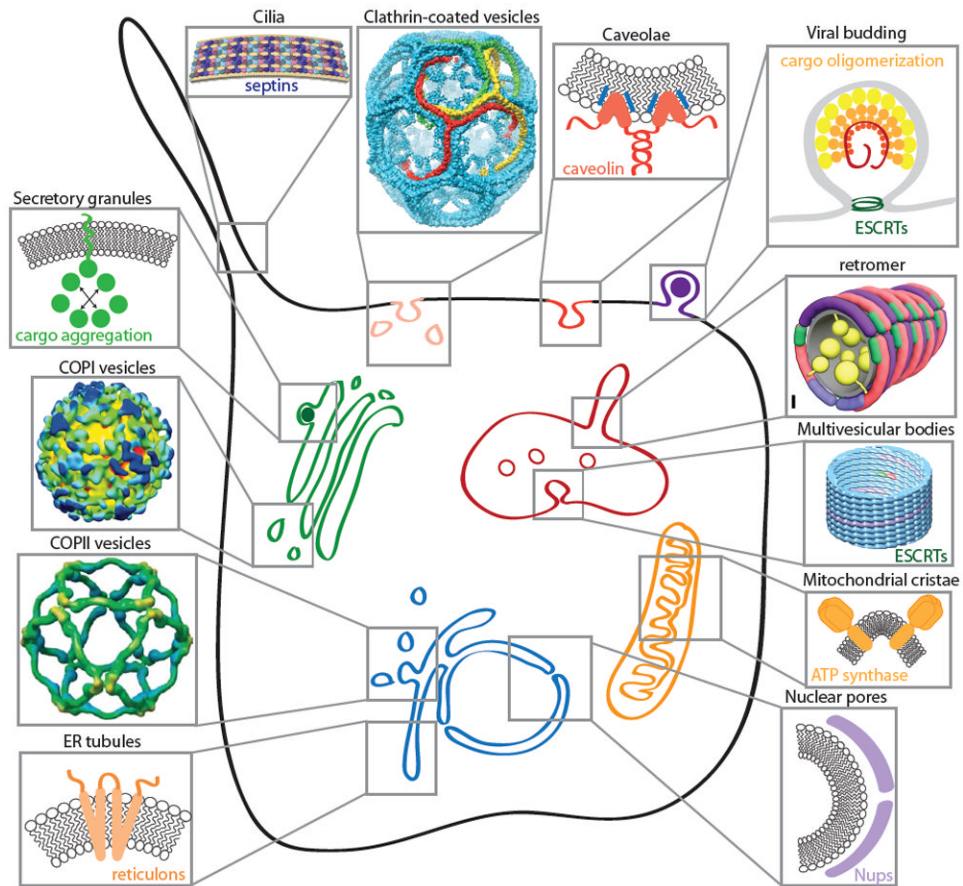


**Figure 1. Cellular sites of membrane curvature**

The membranes of eukaryotic cells display many instances of membrane curvature, some of which are dynamic (e.g. transport vesicles, endosomal tubules, viral buds) and others more static (e.g. nuclear pores, cilia, ER tubules, mitochondrial cristae). Each of these examples of membrane curvature is created by physical effects that derive from both lipid and protein sources. Self-assembling proteins can scaffold membranes (clathrin, COPI, COPII, nucleoporins, caveolins, reticulons, retromer, ESCRTs and septins). Asymmetric lipid and protein insertion can drive curvature by the bilayer couple model and molecular crowding effects (secretory granule cargoes, reticulons, caveolins, viral matrix proteins, mitochondrial ATP synthase). COPI structure reprinted from Faini et al.<sup>46</sup>, copyright 2004, with permission from AAAS. COPII structure reprinted from Stagg et al.<sup>45</sup>, clathrin structure reprinted from Fotin et al.<sup>83</sup>, and retromer model reprinted from Hierro et al.<sup>84</sup>. Septin model reprinted from Tanaka-Takiguchi et al.<sup>85</sup>, copyright 2009, with permission from Elsevier. ESCRT structure reprinted from Effantin et al.<sup>86</sup>, copyright 2013, with permission from Wiley.



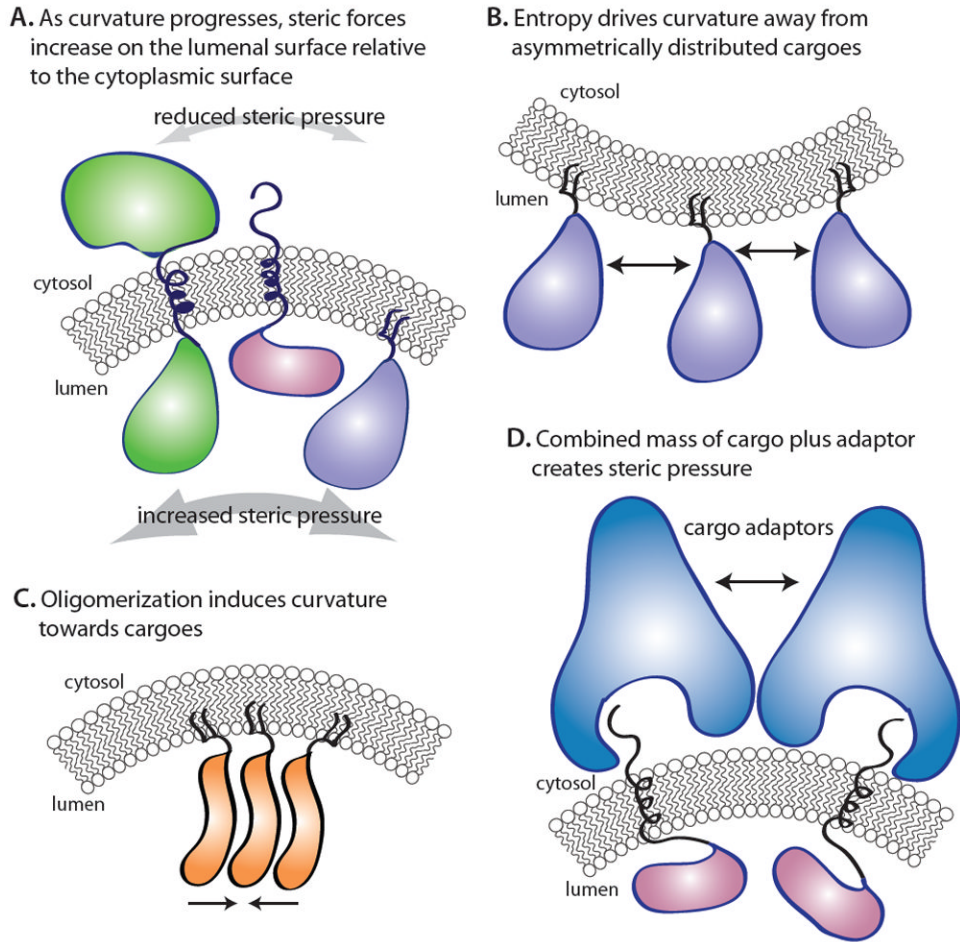


**Figure 2. Steric effects during membrane curvature**

(A) As a vesicle bud forms, the decrease in surface area on the luminal face restricts mobility of luminal protein mass, increasing the local steric pressure to resist bending. Simultaneously, the cytoplasmic surface area increases, reducing steric pressure on this face, necessitating increased force at the cytoplasmic face to maintain bending. (B) Complete asymmetry of lumenally oriented proteins during budding could create negative spontaneous curvature. (C) Conversely to B, if lumenally oriented proteins oligomerize, their affinity for each other and the membrane could drive mending bending in the appropriate direction. (D) Recruitment of cargo adaptors to nascent budding sites could create local curvature by entropic means and reverse cargo resistance.

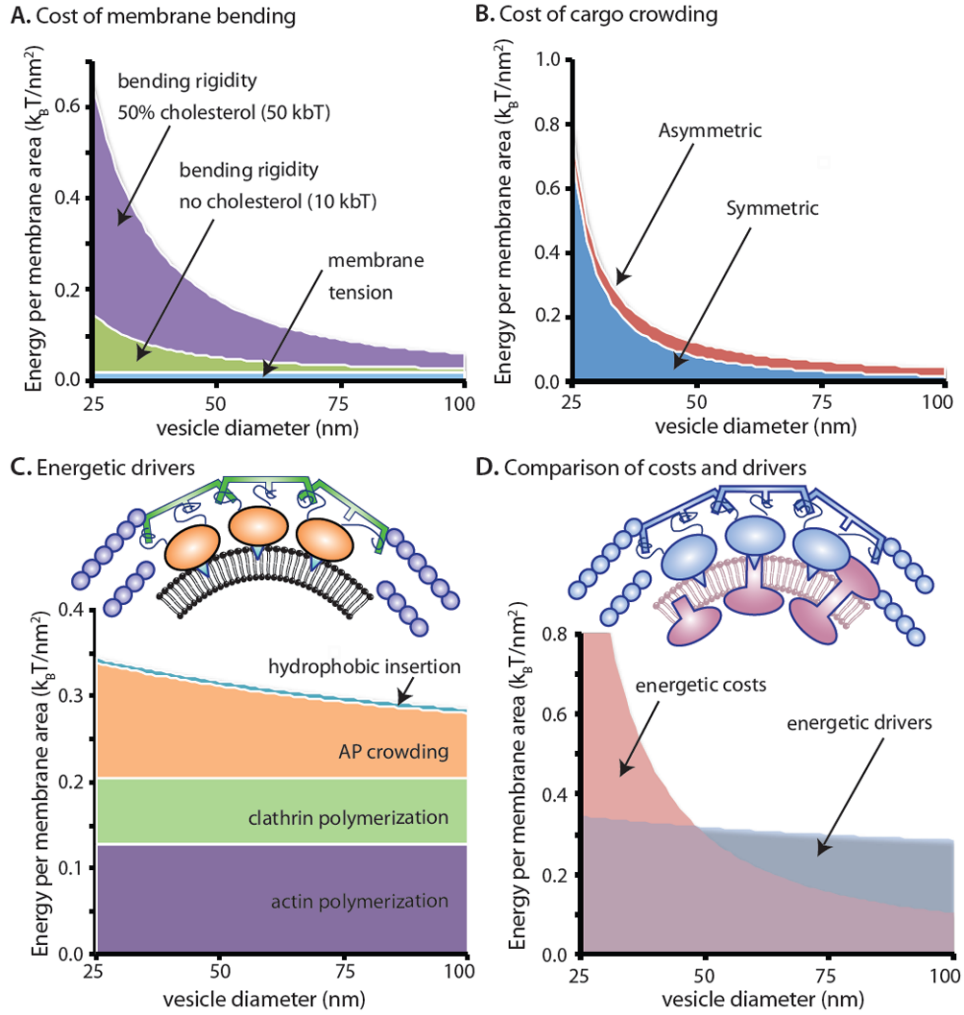


**Figure 3. Energetics of coated vesicle formation**

Compiling quantitative data and models from the recent literature, we estimate the energetic budget responsible for formation of coated vesicles of variable size. (A) Energetic costs of membrane bending including bending rigidity and tension<sup>74</sup>. (B) Energetic costs of cargo confinement in the vesicle lumen<sup>15,31</sup>, (C) Energy contributions by drivers of membrane bending including actin polymerization<sup>7</sup>, clathrin coat assembly<sup>52</sup>, confinement of accessory proteins (AP) beneath coats<sup>31</sup>, and hydrophobic insertions<sup>30</sup>. The colors of each icon correspond to their energetic contributions delineated in the plot. (D) Comparison of energetic costs with energetic drivers during coated vesicle formation. Drivers (actin, clathrin coats and APs) are blue and creating cost-creating cargo are mauve. See Box 1 for further description of these energy estimates.